Volume 22
Number 9
April 27, 1983

Inorganic Chemistry

Contribution from the Department of Chemistry,
Northeastern University, Boston, Massachusetts 02115

Stoichiometry and Kinetics of the Oxidation of Halo(pyridine)copper(I) Complexes by Dioxygen in Aprotic Solvents. Effects of Copper(I) Reactant Molecularity on the Rate Law and Evidence for Ligand-Dependent Product Structures

GEOFFREY DAVIES* and MOHAMED A. EL-SAYED

Received August 31, 1982

The stoichiometry and kinetics of oxidation of L = ethyl nicotinate (ENCA) and L = pyridine (py) complexes of copper(I) chloride and copper(I) bromide by dioxygen have been measured at different molar ratios L/Cu^I_T in methylene chloride and nitrobenzene. Proton magnetic resonance data indicate that ENCA behaves as a monodentate ligand in these systems. Cryoscopic measurements in nitrobenzene solution at $L/Cu^I_T = 2.0$ showed that the proportions of tetrameric $(L_2CuX)_4$ and dimeric $(L_2CuX)_2$ species depend on the total copper(I) concentration, $[Cu^I_T]$. Manometric measurements were consistent with the stoichiometry $\Delta[Cu^I_T]/\Delta[O_2] = 4.0$ under all conditions investigated, demonstrating complete O_2 reduction and ruling out halide, ligand, and solvent oxidation in the presence of excess dioxygen. Cryoscopic measurements established that tetrameric $L_3Cu_4Cl_4O_2$ (L = py) and $L_4Cu_4Cl_4O_2$ (L = ENCA or py) products are formed at $L/Cu^I_T = 0.75$ and $L/Cu^I_T = 1.0$ or 2.0, respectively. Available evidence indicates that $(\mu_4\text{-}O)L_mCu_4X_4O$ (m = 3, 4) products form when L = py, while the $L_4Cu_4X_4O_2$ products with L = *N*,*N*-diethylnicotinamide (DENC) or ENCA have alternative tetrameric $(\mu\text{-}O)_2L_4Cu_4X_4$ core structures. Kinetic measurements with copper(I) in pseudo-first-order excess showed that the oxidation reactions are first order in $[O_2]$, with no spectrophotometric evidence for reactant precursors or reaction intermediates. Tetrameric copper(I) complexes $L_mCu_4X_4$ (L = ENCA, m = 4, X = Cl; m = 8, L = ENCA, py, X = Cl; m = 8, L = ENCA, X = Br) are oxidized with a second-order rate law, $d[L_4Cu_4X_4O_2]/dt = k_T[L_mCu_4X_4][O_2]$, with k_T greatest for oxidation of $(py)_8Cu_4Cl_4$. The kinetic data support insertion of dioxygen into the reactant halo core as the rate-determining step, as previously proposed in $(DENC)_4Cu_4X_4$–dioxygen reactions. By contrast, dimeric $L_4Cu_2Cl_2$ complexes (L = ENCA or py) are oxidized with the overall third-order rate law $d[L_4Cu_4O_2]/dt = k_D[L_4Cu_2Cl_2]^2[O_2]$, k_D being greatest for the oxidation of $(py)_4Cu_2Cl_2$. A mechanism involving rate-determining reaction of a stoichiometrically insignificant $L_4Cu_2Cl_2O_2$ precursor with $L_4Cu_2Cl_2$ is proposed to account for the data. A fourth-order oxidation rate law term $d[L_4Cu_4Cl_4O_2]/dt = k_M[(py)_2CuCl]^3[O_2]$ appears at low relative $[Cu^I_T]$ in methylene chloride, with k_M similar to that for oxidation of $(py)_mCuCl$ in pyridine. The above rate laws imply that irreversible oxidation requires a minimum of three electrons to be transferred from copper(I) to dioxygen in these systems. The relevance of the results to the development of molecular mechanisms for copper-catalyzed oxidative coupling of phenols by dioxygen is discussed.

Introduction

The oxocopper(II) products of aprotic oxidation of slurried copper(I) chloride by dioxygen in pyridine initiate the copper-catalyzed oxidative coupling of phenols under ambient conditions (eq 1).[1] This discovery has been put to good use

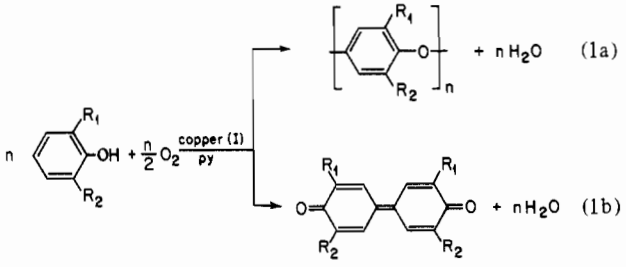

in developing a range of commercial poly(phenylene oxide) materials with outstanding electrical and thermal properties.[2]

Published work on the extension of reaction 1 to other oxidative coupling systems primarily describes (a) experimental conditions (ligands, solvents, substrates, etc.) that affect the rate of dioxygen consumption and the yield and molecular weight distributions of the polymeric products[3] and (b) the mechanism of polymer growth.[4]

In recent years attention increasingly has been focused on the likely coordination and redox properties of the copper–oxygen intermediates involved in the catalytic steps:[5-7] the findings and conclusions are relevant to the mechanisms of all copper-catalyzed reactions of dioxygen.[7] Although no complete kinetically established phenolic oxidative coupling

(1) Hay, A. S.; Blanchard, H. S.; Endres, G. F.; Eustance, J. W. *J. Am. Chem. Soc.* **1959**, *81*, 6335.
(2) Hay, A. S.; Shenian, P.; Gowan, A. C.; Erhardt, P. F.; Haaf, W. R.; Therberg, J. E. in "Encyclopedia of Polymer Science and Technology"; Interscience: New York, 1969; p 92.
(3) Finkbeiner, H. L.; Hay, A. S.; White, D. M. In "Polymerization Processes"; Schildnecht, C. E., Skeist, I., Eds.; Wiley-Interscience: New York, 1977; pp 537–581.
(4) White, D. M. *J. Org. Chem.* **1969**, *34*, 297.
(5) Rogić, M. M.; Demmin, T. R. *J. Am. Chem. Soc.* **1978**, *100*, 5472. Rogić, M. M.; Demmin, T. R. in "Aspects of Mechanism in Organometallic Chemistry"; Brewster, J. H., Ed.; Plenum Press: New York, 1978; p 141. Demmin, T. R.; Rogić, M. M. *J. Org. Chem.* **1980**, *45*, 1153, 2737, 4210; Demmin, T. R.; Swerdloff, M. D.; Rogić, M. M. *J. Am. Chem. Soc.* **1981**, *103*, 5795.
(6) Parshall, G. W. "Homogeneous Catalysis"; Wiley-Interscience: New York, 1980; p 133.
(7) Gampp, H.; Zurberbühler, A. D. *Met. Ions Biol. Syst.* **1981**, *12*, 133.

0020-1669/83/1322-1257$01.50/0

mechanism is yet available, it seems likely from previous work that (phenolato)copper(II) complexes participate and that inner-sphere electron transfer from phenol to copper(II) occurs at least under some experimental conditions.[5-8]

Dioxygen is completely reduced by simple copper(I) complexes under aprotic conditions.[9,10] The highly reactive oxocopper(II) products, whose stability, proton basicity, and other properties depend on their ligand–solvent environment,[9-11] often initiate phenolic oxidative coupling reactions, presumably by deprotonating neutral phenol molecules and thereby facilitating their electron transfer to copper(II).[7,12] Because the copper(I) centers resulting from this initiation step are formed in the presence of a large excess of phenol, their structures may not be the same as that of the copper(I) complex used to generate the initiator. Phenol coordination by copper(I) might alter the mechanism of its reaction with dioxygen by affecting the reactant molecularity.[7,13]

Progress has been made in establishing the underlying aprotic copper(I)–dioxygen chemistry in the absence of substrates.[7,9,10] The fundamental problem in work addressing catalytic mechanisms is the discovery of soluble copper(I) reactant complexes that give discrete, soluble, and stable oxocopper(II) products.[9] For example, although soluble alkylpolyaminecopper(I) complexes are rapidly oxidized by dioxygen, the highly active oxocopper(II) initiator products seem always to be polymeric $(L_mCu_2X_2O)_n$ species,[14] leading to complications when they are used for separate kinetic studies of reactions with phenols.

A recent paper from our research group[15] reported stoichiometric and kinetic data for reactions of tetranuclear $[(DENC)CuX]_4$ complexes (DENC = *N*,*N*-diethylnicotinamide; X = Cl, Br) with dioxygen in anhydrous benzene,

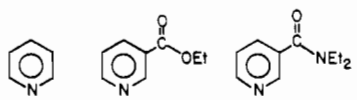

Py ENCA DENC

methylene cloride, and nitrobenzene solvents (eq 2). The

$$[(DENC)CuX]_4 + O_2 \rightarrow [(DENC)CuX]_4O_2 \quad (2)$$

stoichiometry of eq 2 indicates that no ligand or solvent oxidation takes place,[9] and X-ray structural and spectral data showed that DENC is only bound through its pyridine nitrogen atom in the reactant and product.[15] The brown tetranuclear species $[(DENC)CuX]_4O_2$ are stable either as solids or in solution in the absence of moisture; although they have not yet been obtained in crystalline form, stoichiometric reaction 3 suggests that they contain equivalent (μ-oxo)copper(II) units (see Results and Discussion).[15,16]

$$[(DENC)CuX]_4O_2 + 2CO_2 \rightarrow [(DENC)CuX]_4(CO_3)_2 \quad (3)$$

No reactant preequilibria or reaction intermediates were detected in kinetic studies of reactions 2, which follow a simple second-order rate law (eq 4), where k_T is the second-order rate

$$d[[(DENC)CuX]_4O_2]/dt = k_T[[(DENC)CuX]_4][O_2] \quad (4)$$

constant. With X = Cl, k_T exhibited hardly any solvent dependence, making a polar transition state appear unlikely. Activation entropies were in the range −40 to −48 cal deg^{-1} mol^{-1}, suggesting an associative mechanism. The rate constant k_T decrease with a change from X = Cl to X = Br in nitrobenzene was solely due to an increase in $\Delta H_T^{\ddagger}$ from 3.9 to 5.9 kcal mol^{-1}.[15]

A mechanism involving rate-determining insertion of dioxygen into the tetrahedral core of halogen atoms in $[(DENC)CuX]_4$ was proposed to account for these results.[15] Rapid electron transfer to dioxygen evidently follows this rate-determining step, presumably because the four electrons required for complete dioxygen reduction are available in one molecular unit.

This paper reports stoichiometric and kinetic data for the oxidation of pyridine- and (ENCA)–copper(I) halide complexes by dioxygen in methylene chloride and nitrobenzene, where ENCA = ethylnicotinate and X = Cl, Br. These ligands also stabilize tetranuclear oxocopper(II) products, but the product with pyridine appears to have a core structure that differs from those with DENC and ENCA. The kinetic data for reactions with pyridine and ENCA as ligands support the insertion mechanism for aprotic oxidation of tetranuclear copper(I) halide complexes by dioxygen.[15] In addition, under particular experimental conditions and unlike the case with DENC, these ligands promote the formation of dimeric and monomeric copper(I) complexes. As will be seen, the rate law for copper(I) oxidation is a reflection of the copper(I) reactant molecularity.

Experimental Section

Materials. Pyridine, py (Aldrich), was dried over potassium hydroxide for 24 h and then distilled from BaO and stored in the dark over 4-Å molecular sieves. ENCA (Aldrich) was dried over 4-Å molecular sieves and distilled under reduced pressure immediately before use. Copper(I) halides were prepared by literature methods.[17] Nitrobenzene (Aldrich) was distilled over P_2O_5 at reduced pressure and stored over 4-Å molecular sieves. The purifications of benzene, carbon dioxide, diethyl ether, 2,6-dimethylphenol, methylene chloride, and dinitrogen were carried out as previously described.[15,16]

Synthetic Methods. The complexes $[LCuX]_4$, where L = py, ENCA and X = Cl, Br, I, were prepared in methylene chloride or nitrobenzene as previously described for L = DENC.[15] The air-sensitive products with X = Cl, Br were always much less soluble than the corresponding DENC complexes, with the ENCA–chloride combination giving the most soluble complex at molar ratio $L/Cu^I_T = 1.0$. With L = py at $L/Cu^I_T = 0.75$ or 1.0, the copper(I) products with X = Cl, Br were virtually insoluble in methylene chloride and nitrobenzene, precluding subsequent kinetic measurements of their homogeneous reactions with dioxygen but not preventing identification of the much more soluble products. Higher copper(I) complex solubilities were observed with molar reactant ratios $L/Cu^I_T = 2.0$, and with X = Cl the products were freely soluble in methylene chloride and nitrobenzene. Cryoscopic measurements in dioxygen-free nitrobenzene were used to identify the predominant copper(I) species under various experimental conditions.

As found for $[(DENC)CuX]_4$ complexes with X = Cl, Br,[15] the solid products isolated from experiments at $L/Cu^I_T = 1.0$, 2.0 were too air-sensitive to give reliable elemental analyses or disk IR spectral data.

Stoichiometry and Products of Reactions of $[L_mCuX]_n$ Complexes with Dioxygen (L = py, ENCA; $m = 1$, $n = 4$ and $m = 2$, $n = 2, 4$; X = Cl, Br). The stoichiometries of the rapid oxidations of mixtures of ligands and copper(I) halides with dioxygen, at the molar stoichiometries given in this section heading, were measured manometrically[15] over a range of concentrations in nitrobenzene and methylene

(8) Carr, B.; Harrod, J. F. *J. Am. Chem. Soc.* **1973**, *95*, 5707 and references therein.
(9) Davies, G.; El-Shazly, M. F.; Kozlowski, D. R.; Kramer, C. E.; Rupich, M. W.; Slaven, R. W. *Adv. Chem. Ser.* **1979**, *No. 173*, 178.
(10) Davies, G.; El-Sayed, M. A. "Biochemical and Inorganic Perspectives in Copper Co-ordination Chemistry"; Karlin, K. D., Zubieta, J. A., Eds.; Adenine Press: Guilderland, NY, in press.
(11) See, for example: Bodek, I.; Davies, G. *Inorg. Chim. Acta* **1978**, *27*, 213.
(12) Davies, G.; El-Shazly, M. F.; Rupich, M. W. *Inorg. Chem.* **1981**, *20*, 3757.
(13) Price, C. C.; Nakaoka, K. *Macromolecules* **1971**, *4*, 363.
(14) Churchill, M. R.; Davies, G.; El-Sayed, M. A.; El-Shazly, M. F.; Hutchinson, J. P.; Rupich, M. W. *Inorg. Chem.* **1981**, *20*, 201.
(15) Churchill, M. R.; Davies, G.; El-Sayed, M. A.; Hutchinson, J. P.; Rupich, M. W. *Inorg. Chem.* **1982**, *21*, 995.
(16) Churchill, M. R.; Davies, G.; El-Sayed, M. A.; Hutchinson, J. P. *Inorg. Chem.* **1982**, *21*, 1002.
(17) Keller, R. N.; Wycoff, H. D. *Inorg. Synth.* **1946**, *2*, 1. Glemser, O.; Sauer, H. "Handbook of Preparative Inorganic Chemistry"; Brauer, G., Ed.; Academic Press: New York, 1965; Vol. 2, p 1006.

Table I. Analytical and Cryoscopic Data

complex	anal. calcd, found					
	% C	% H	% N	% other		mol wt
$(ENCA)_4Cu_2Cl_2$[a]						802, 700 ± 50[b]
$(ENCA)_8Cu_4Cl_4$[a]						1604, 1500 ± 100[c]
$(py)_4Cu_2Cl_2$[a]						514, 470 ± 20[d]
$(py)_8Cu_4Cl_4$[a]						1028, 1010 ± 20[e]
$[(ENCA)CuCl]_4O_2$	37.2, 35.4	3.5, 3.7	5.4, 5.2	24.6,[f] 25.7	13.8,[g] 14.7	324, 300 ± 25[h]
$[(ENCA)CuBr]_4O_2$	31.8, 30.5	3.0, 3.0	4.6, 4.4	21.0,[f] 21.6	26.4,[g] 26.4	
$[(ENCA)CuCl]_4(CO_3)_2$	36.4, 35.0	3.2, 3.5	5.0, 4.9	12.7,[g] 14.5		1121, 950 ± 50
$(py)_3Cu_4Cl_4O_2$						665, 590 ± 20[i]
$(py)_4Cu_4Cl_4O_2$						744, 733 ± 20[j]
$(py)_4Cu_4Cl_4O_2$						257, 250 ± 10[k]
$(py)_4Cu_4Cl_6O$[l]	30.0, 32.4	2.5, 2.7	7.0, 7.4	31.8,[f] 30.2	26.7,[g] 26.6	
$(DENC)_4Cu_4Cl_6(OH)_2$[l]	39.6, 38.8	4.6, 4.8	9.2, 9.0	17.6,[f] 17.8		

[a] These complexes are too dioxygen sensitive to give reliable analytical data. [b] Measured at $ENCA/Cu^I_T = 2.0$ with formal copper(I) molality 4.0×10^{-2}. [c] Measured at $ENCA/Cu^I_T = 2.0$ with formal copper(I) molality 26.8×10^{-2}. [d] Measured at $py/Cu^I_T = 2.0$ with formal copper(I) molality 1.4×10^{-2}. [e] Measured at $py/Cu^I_T = 2.0$ with formal copper(I) molality 27.0×10^{-2}. [f] Copper. [g] Halide. [h] Solutions in footnotes *b* and *c* were stoichiometrically oxidized with dioxygen; results correspond to the presence of 1 mol of $[(ENCA)CuCl]_4O_2$ and 4 mol of free ENCA under both conditions (see eq 5). [i] Measured at $py/Cu^I_T = 0.75$ with formal copper(II) molality 2.0×10^{-2}. [j] Measured at $py/Cu^I_T = 1.0$ with formal copper(II) molality 2.0×10^{-2}; analytical data are given in ref 23. [k] Solution at $py/Cu^I_T = 2.0$ was stoichiometrically oxidized with dioxygen at formal copper(I) molality 2.0×10^{-2}; result corresponds to the presence of 1 mol of $(py)_4Cu_4O_2$ and 4 mol of free py (see eq 5). [l] Disproportionation products: see text.

chloride. Studies were also made of the heterogeneous system with $py/Cu^I_T = 0.75$ (see Results and Discussion). Solid products were obtained from nitrobenzene solutions by pouring them into a large excess of anhydrous hexane or diethyl ether. The brown precipitates were subsequently washed with hexane and dried overnight under vacuum. Analytical data[18] for the same solids obtained by evaporation of methylene chloride product solutions at $ENCA/Cu^I_T = 1.0$, together with cryoscopic data for oxidized solutions in nitrobenzene at $ENCA/Cu^I_T = 2.0$, are collected in Table I. Elemental analytical data for the solid products obtained with L = py at $L/Cu^I_T = 0.75$ and $L/Cu^I_T = 1.0$ were unacceptably irreproducible, and so the species present in oxidized nitrobenzene solution at these respective molar ratios were determined cryoscopically (Table I). The cryoscopic data show that the oxocopper(II) products are all tetranuclear.

Synthesis of $[(ENCA)CuCl]_4(CO_3)_2$. The previously described procedure[16] was used to obtain this complex. Analytical data are given in Table I.

Physical Measurements. Solution electronic spectral measurements were made with Cary 14 and Beckman DK-1A spectrophotometers in matched quartz cells at room temperature. Infrared spectra, either in KBr disks or in solution, were obtained with a Perkin-Elmer Model 567 spectrometer calibrated with the 906.5- or 3026.3-cm^{-1} absorptions of polystyrene. ^1H NMR spectra were observed with a JEOL Model FX60Q spectrometer at 25 °C with tetramethylsilane as internal reference. The magnetic susceptibilities of oxidation products were obtained with a PAR Model FM-1 vibrating-sample magnetometer calibrated with $HgCo(SCN)_4$. Powder and glassy-solution ESR spectra were measured with a Varian E-9 spectrometer at 77 K.

Kinetic Measurements. Kinetic measurements of reactions of copper(I) complexes with dioxygen were always conducted with copper(I) in sufficient excess to ensure pseudo-first-order conditions. This choice of conditions, which is based on our previous experience with DENC,[15] restricted the number of homogeneous systems that could be investigated due to the lower copper(I) complex solubilities allowed by py and ENCA ligands (a range of copper(I) concentrations was needed for reliable determination of reaction orders; see below).

The rates of formation of $[LCuX]_4O_2$ products (L = py, ENCA; X = Cl, Br) on mixing homogeneous solutions of copper(I) complexes and dioxygen were monitored spectrophotometrically in the wavelength range 500–850 nm. The Beckman spectrophotometer, fitted with a cell housing maintained to within ±0.1 °C of the desired temperature, was used for X = Br; the experimental procedure has been described.[15] A computer-assisted stopped-flow spectrophotometer[19] was employed for rapid rate measurements with X = Cl, at temperatures controlled to within ±0.05 °C of the desired value.

The excess copper(I) reactant concentrations leading to particular rate laws in reactions with dioxygen are given in the Results and Discussion section. In each run the experimental O_2 concentration was determined from the absorption, A_∞, after at least 10 half-lives by dividing it by the molar absorptivity of the $[LCuX)_4O_2$ product (see eq 2; the copper(I) reactants have negligible absorbance at the wavelengths used for $[O_2]$ determinations).

Table II. Cryoscopic Data at $ENCA/Cu^I_T = 2.0$ in Nitrobenzene

$10^2 \times [Cu^I_T]$[a]	mol wt calcd, found	$10^2 \times [Cu^I_T]$[a]	mol wt calcd, found
1.66	802,[b] 700 ± 50	11.2	1604,[c] 1500 ± 30
4.0	802,[b] 710 ± 30	26.8	1604,[c] 1510 ± 25

[a] Total formal copper(I) molality (equal to 2 times dimer molality or 4 times tetramer molality). [b] Calculated for $(ENCA)_4Cu_2Cl_2$. [c] Calculated for $(ENCA)_8Cu_4Cl_4$.

Results and Discussion

Identification of Copper(I) Reactants. Ligand Binding Mode. In previous work[15] we established from the crystal structure and IR spectrum of air-stable $[(DENC)CuI]_4$ that the DENC ligand is coordinated only through its pyridine ring nitrogen atom. Molecular weight measurements in nitrobenzene and ^1H NMR spectra for free DENC and $[(DENC)CuX]_4$ (X = Cl, Br) in $CDCl_3$ confirmed that these complexes are tetranuclear with monodentate, pyridine-*N* coordinated ligands.

The ENCA complexes formed at $L/Cu^I_T = 1.0$ are more air-sensitive but much less soluble than their DENC analogues, precluding precise IR, ^1H NMR, and cryoscopic measurements. However, at $ENCA/Cu^I_T = 2.0$, where solubility is much greater, molecular weight measurements established a tetranuclear structure (Table I) and proton chemical shifts[15] (methylene, 3.71, 4.46, 4.28; methyl, 1.22, 1.46, 1.29 ppm vs. TMS) for ENCA, $[(ENCA)_2CuCl]_4$, and $[(ENCA)_2CuBr]_4$, respectively, were very similar, ruling out coordination of the ester substituent. These conclusions are supported by second-order kinetics for the reactions of dioxygen with ENCA–copper(I) complexes at $ENCA/Cu^I_T = 1.0$ and $ENCA/Cu^I_T = 2.0$ (the latter at high relative total copper(I) concentrations, see below).

Reactant Molecularities. Table II lists apparent molecular weights for $Cl(ENCA)_2Cu^I$ species at different total copper(I) concentrations, $[Cu^I_T]$. It is evident that dimeric complexes $(ENCA)_4Cu_2Cl_2$ form at lower $[Cu^I_T]$. These changes in molecularity are reflected by a change of order in the kinetics of reaction with dioxygen over similar concentration ranges (see below).

(18) All elemental analyses were performed by Galbraith Laboratories, Knoxville, TN.
(19) Bodek, I.; Davies, G. *Inorg. Chem.* **1978**, *17*, 1814.

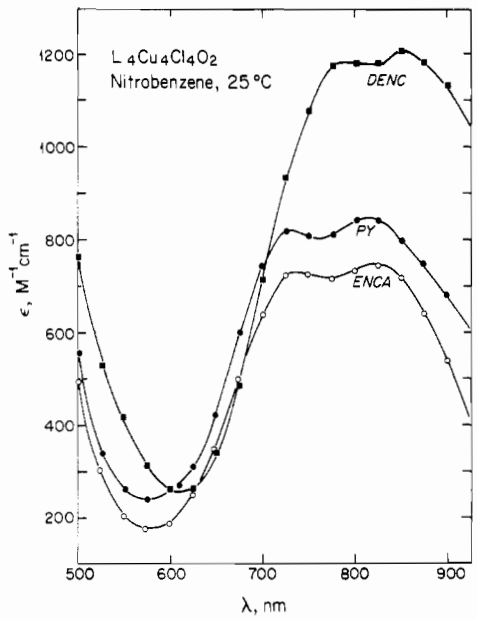

Figure 1. Room-temperature electronic spectra for $L_4Cu_4Cl_4O_2$ oxidation products.

Pyridine–copper(I) halide complexes are even less soluble in methylene chloride and nitrobenzene than the corresponding ENCA species, precluding cryoscopic molecular weight and kinetic measurements at $py/Cu^I_T = 1.0$. However, molecular weight mesurements on near-saturated nitrobenzene solutions at [py]/[CuCl] = 2.0 at ~7 °C (that is, near the freezing point of nitrobenzene[14]) showed the existence of tetramers, while dimers were found to be predominant at lower total copper(I) concentrations (Table I). An increase of solubility with increasing temperature enabled kinetic measurements to be made at copper(I) concentrations higher than those at 7 °C, and rate laws characteristic of reactions of tetrameric $[(py)_2CuCl]_4$ species were observed under these conditions.

In summary, it seems clear that L = ENCA and DENC[15] both behave as monodentate ligands for copper(I) halides at $L/Cu^I_T = 1.0$ or 2.0. Because of solubility limitations and air sensitivity we have not been able to confirm the existence of $[LCuX]_4$ complexes (L = py, ENCA; X = Cl, Br) independently, although this was found practical with L = DENC.[15] It has, however, been possible to identify the following species cryoscopically: $[(ENCA)_2CuCl]_4$, $[(ENCA)_2CuCl]_2$, $[(py)_2CuCl]_4$, and $[(py)_2CuCl]_2$. Since $[(DENC)CuI]_4$ and $[pyCuI]_4$ have virtually identical "cubane" core structures,[15] it is reasonable to suppose that this is the case for all $[L_mCuX]_4$ species (L = a monodentate pyridine; m = 1, 2). The kinetic results presented below support this conclusion. The dimeric $L_4Cu_2Cl_2$ species that we have detected presumably have a bis(μ-halo)-bridged structure like that established in $(teed)_2Cu_2Br_2$ (teed = *N,N,N',N'*-tetraethylethylenediamine).[20]

Stoichiometries and Products of Oxidation. Manometric measurements of dioxygen consumption established that four copper(I) centers are stoichiometrically oxidized by one dioxygen molecule under all experimental conditions, consistent with the results obtained previously in pyridine[19] and with DENC as ligand (eq 2).[15] These results rule out halide, ligand, and solvent oxidation by excess dioxygen in the presence of the oxocopper(II) products.[9]

The visible spectra for nitrobenzene solutions of products obtained with L = py, ENCA and X = Cl at $L/Cu^I_T = 1.0$ are compared with that of $[(DENC)CuCl]_4O_2$ in Figure 1. These distinctive spectra and associated high molar absorptivities are characteristic of tetranuclear $L_4Cu_4X_4O_2$ oxocopper(II) complexes, as indicated by the analytical data in Table I.[15,18]

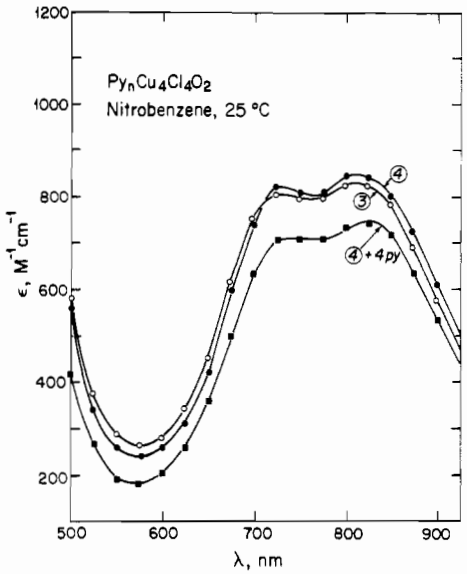

Figure 2. Room-temperature electronic spectra for $py_nCu_4Cl_4O_2$ oxidation products, n = 3 and 4. The lowest spectrum was for a solution obtained by oxidation of $[(py)_2CuCl]_4$ with O_2. Cryoscopic (Table I) and spectral measurements show that it corresponds to 1 mol of $(pyCuCl)_4O_2$ and 4 mol of free pyridine involved in equilibrium 6.[21]

Dissimilar results were obtained with L = DENC, ENCA, py at L/Cu^I_T 0.75. For L = DENC or ENCA, only 75% of the same $L_4Cu_4X_4O_2$ product was obtained (that is, 25% of the initial copper(I) halide remained as an unreactive solid (determined gravimetrically), whereas with L = py no solid copper(I) halide remained after stoichiometric dioxygen consumption). The cryoscopic data in Table I show that the product obtained at $py/Cu^I_T = 0.75$ with X = Cl is $(py)_3Cu_4Cl_4O_2$, whose spectrum is virtually identical with that of $(py)_4Cu_4Cl_4O_2$ (Figure 2).

The pyridine ligand system also gives results different from those with L = DENC and ENCA at $L/Cu^I_T = 2.0$. For all three ligands the nitrobenzene product solutions obtained by complete oxidation behave cryoscopically as if they contain 1 mol of $L_4Cu_4X_4O_2$ and 4 mol of free ligand (Table I and eq 5). The product spectra obtained with DENC and ENCA

$$L_8Cu_4X_4 + O_2 \rightarrow L_4Cu_4X_4O_2 + 4L \qquad (5)$$

ligands were identical with those of $L_4Cu_4X_4O_2$ (Figure 1), and they were virtually identical in methylene chloride and nitrobenzene. However, the spectrum of $(py)_4Cu_4X_4O_2$ differs significantly in nitrobenzene (Figure 2) and methylene chloride (λ_{max} = 725 nm (ϵ 725 M^{-1} cm^{-1}) and λ_{max} 812 nm (ϵ 715 M^{-1} cm^{-1})) and the product spectrum at $py/Cu^I_T = 2.0$ differs from that at $py/Cu^I_T = 0.75$ and 1.0 (Figure 2).

In summary, $L_4Cu_4X_4O_2$, L = ENCA, DENC and X = Cl, Br, are the only oxidation products from the corresponding $L_4Cu_4X_4$ or $L_8Cu_4X_4$ systems; their visible spectra are solvent independent and are not affected by fourfold excesses of free ligand. By contrast, although $(py)_4Cu_4X_4O_2$ is the predominant product of oxidation at $py/Cu^I_T = 1.0$ or 2.0, its spectrum is solvent dependent and sensitive to the presence of a fourfold excess of free pyridine. Subsequent experiments have shown that reaction 6 takes place on addition of more free pyridine

$$(py)_4Cu_4X_4O_2 + 4py \rightleftarrows 2(py)_2CuX_2 + (py)_4Cu_2O_2 \qquad (6)$$

to these oxidized solutions.[21] The products of reaction 6 are

(20) Churchill, M. R.; Davies, G.; El-Sayed, M. A.; Fournier, J. A.; Hutchinson, J. P., submitted for publication.

(21) Davies, G.; El-Sayed, M. A.; Fasano, R. *Inorg. Chim. Acta* **1983**, *71*, 95.

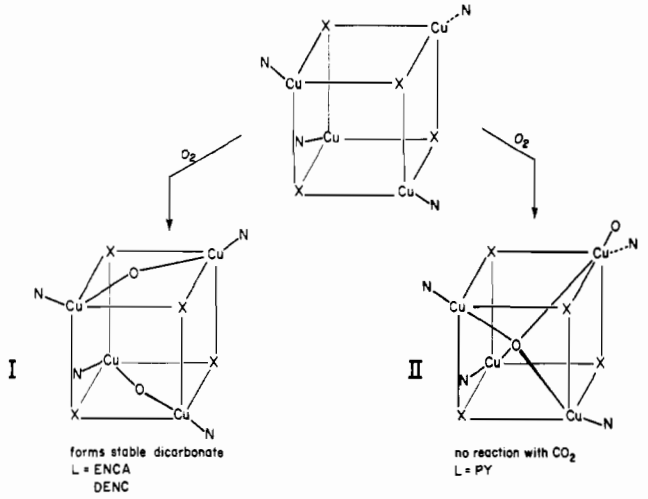

Figure 3. Proposed alternative (μ-oxo)tetracopper(II) products from the reactions of $(LCuX)_4$ complexes with dioxygen. Note the unlikely formation of a chelated carbonato structure for the μ_4-oxo product II.[14]

spectrally and chromatographically identical with those obtained by oxidation of copper(I) halide slurries in neat pyridine.[19,21]

The monodentate coordination of ENCA via its pyridine-*N* atom is confirmed by no difference in ν_{CO} absorption at 1725 cm^{-1} between free ENCA and $[(ENCA)CuX]_4O_2$. As found with $[(DENC)CuX]_4O_2$ (Table VII of ref 15), the IR bands associated with the pyridine rings of ENCA are shifted to higher frequency in $[(ENCA)CuX]_4O_2$; the medium-intensity band centered at 555 cm^{-1} may be assigned to ν_{CuO}.[15]

Despite numerous attempts, none of the products $L_4Cu_4X_4O_2$ (L = DENC, ENCA, py) or $(py)_3Cu_4X_4O_2$ have yet been obtained in crystalline form. However, the following evidence leads us to conclude that they have the different core structures given in Figure 3.

(1) The stoichiometry $(py)_3Cu_4Cl_4O_2$ is reminiscent of those of the $L_3Cu_4X_4O_2$ products obtained by copper halide slurry oxidation in L = dimethylacetamide, dimethyl sulfoxide, and *N*-methyl-2-pyrrolidinone, nmp.[9,22] The spectral properties of $(nmp)_3Cu_4Cl_4O_2$ and its crystalline disproportionation derivative $(nmp)_3Cu_4Cl_6O(OH_2)\cdots nmp$ are very similar,[22] indicating that the former almost certainly contains a μ_4-oxo core.

(2) The ESR spectra of $(nmp)_3Cu_4Cl_4O_2$ ($g_\parallel$ = 2.37 and $g_\perp$ = 2.08)[22] and $(py)_3Cu_4Cl_4O_2$ ($g_\parallel$ = 2.260 and $g_\perp$ = 2.050)[23] are very similar, whereas $[(DENC)CuCl]_4O_2$ and $[(ENCA)CuCl]_4O_2$ are both ESR silent.

(3) Analogies between $(nmp)_3Cu_4X_4O_2$ and $(py)_3Cu_4X_4O_2$ core structures also are supported by the fact that both are initiators for reaction 1b, whereas $L_4Cu_4X_4O_2$ complexes (L = DENC, ENCA; X = Cl, Br) are inactive. The site of oxidative coupling initiation is the terminal oxo group in structure II,[22] which would be expected to be more basic[7] than the μ-oxo sites in structure I, particularly when we realize that DENC and ENCA are probably stronger π acids than either py or nmp (see below).

(4) Neither $(nmp)_3Cu_4Cl_4O_2$ nor $(py)_3Cu_4X_4O_2$ react in solution with excess CO_2, whereas $L_4Cu_4X_4O_2$ (L = DENC,[16] ENCA) quantitatively form dicarbonato complexes (eq 3 and Table I). The μ_4-oxo core of structure II is inaccessible to reaction with CO_2, and reaction with the terminal oxo group would only give a weak monodentate carbonato complex: the O–Cu–O unit in $(\mu_4\text{-O})(nmp)_3Cu_4Cl_6(OH_2)\cdots nmp$ is linear,[22] which would require very long bonds Cu···OC(O)O···Cu in $(\mu_4\text{-O})(py)_3Cu_4X_4{\cdot}CO_3$ if the carbonate group were to be chelated in a surviving tetranuclear structure (structure II of Figure 3).

(5) The visible spectra of $(py)_3Cu_4X_4O_2$ and $(py)_4Cu_4X_4O_2$ are solvent dependent, consistent with polar structure II and not anticipated or found for symmetrical structure I.

(6) The disproportionation products obtained on attempted crystallization of these primary oxocopper(II) products are different. As detailed elsewhere,[22] $(nmp)_3Cu_4Cl_4O_2$ gives crystalline $(\mu_4\text{-O})(nmp)_3Cu_4Cl_6(OH_2)\cdots nmp$, via eq 7, on

$$3(nmp)_3Cu_4Cl_4O_2 + 6H_2O \xrightarrow{nmp} 2(\mu_4\text{-O})(nmp)_3Cu_4Cl_6(OH_2)\cdots nmp + 4nmpCu(OH)_2 \quad (7)$$

attempted crystallization from nmp solvent. Analytical data for crystalline products of disproportionation of $[(DENC)CuX]_4Y_2$ (X = Cl, or Br; Y = O or CO_3), which obeys the stoichiometry of eq 7, are given in Table I. Although these crystals are too small for single-crystal X-ray structural work, their spectral and other properties suggest their formulation as dihydroxo complexes, $(DENC)_4Cu_4Cl_6(OH)_2$, rather than as the (μ_4-oxo)aquo structure known[22] for the first product of eq 7. By contrast, crystralline $(\mu_4\text{-O})(py)_4Cu_4X_6$ (X = Cl or Br), identified by comparison with authentic samples[24] and an independent crystal structure determination of $(\mu_4\text{-O})(py)_4Cu_4Br_6$,[25] is obtained on attempted crystallization of $(py)_mCu_4X_4O_2$ (m = 3 or 4) from nitrobenzene or methylene chloride (Table I).

Table III. Magnetic Moments (μ_{eff}, 298 K) for Oxidation and Disproportionation Products

complex	μ_{eff}, μ_B	complex	μ_{eff}, μ_B
$[(DENC)CuCl]_4O_2$	1.69	$[(ENCA)CuCl]_4O_2$	1.70
$[(DENC)CuBr]_4O_2$	1.40	$[(ENCA)CuBr]_4O_2$	1.72
$[(DENC(CuCl]_4(CO_3)_2$	1.70[a]	$[(ENCA)CuCl]_4(CO_3)_2$	2.05
$[(DENC)CuBr]_4(CO_3)_2$	1.59	$(py)_4Cu_4Cl_6O$	1.54
$(DENC)_4Cu_4Cl_6(OH)_2$	2.05[a]	$(py)_4Cu_4Br_6O$	2.05

[a] Temperature independent, $80 \leq T \leq 300$ K.

Magnetic Properties. The magnetic moments at 25 °C of oxidation products and their derivatives are collected in Table III. The strongest antiferromagnetic interactions between metal centers are found in $[(DENC)CuBr]_4Y_2$ (Y = O, CO_3). The magnetic moments of $[(DENC)CuCl]_4(CO_3)_2$ and $[(DENC)_4Cu_4Cl_6](OH)_2$ are temperature independent in the range $80 \leq T \leq 300$ K. We are currently investigating temperature dependences in the other systems.

The conclusion that both $(py)_3Cu_4X_4O_2$ and $(py)_4Cu_4X_4O_2$ have core structure II has historical significance. First, we had demonstrated the tendency for polymerization of "CuO" species from the reaction of slurried copper(I) halides in pyridine with dioxygen[19] and have subsequently found that the same species can be generated on treatment of $(py)_4Cu_4X_4O_2$ with py (eq 6).[21] It is easy to see that breakdown of structure II via eq 6 would produce a pyCu–O–Cu(py)–O species, which would readily polymerize to form $[(py)_mCu_2O_2]_n$ because of its nucleophilic terminal oxo group. Second, we had labored for years under the mistaken impression that a large excess of pyridine was necessary to stabilize soluble initiators of stoichiometry Cu/O = 1.0.[9,19] It is now clear that copper(II)–halide bridging in $(py)_mCu_4X_4O_2$ species helps to stabilize them even at m = 3 and that they break down in the presence

(22) Davies, G.; El-Shazly, M. F.; Rupich, M. W.; Churchill, M. R.; Rotella, F. J. *J. Chem. Soc., Chem. Commun.* **1978**, 1045. Churchill, M. R.; Rotella, F. J. *Inorg. Chem.* **1979**, *18*, 853. Rupich, M. W. Doctoral Dissertation, Northeastern University, 1980.

(23) Praliaud, H.; Kodratoff, Y.; Coudurier, G.; Mathieu, M. V. *Spectrochim. Acta, Part A* **1974**, *30A*, 1389.

(24) Dieck, H. T. *Inorg. Chim. Acta* **1973**, *7*, 397 and references therein.

(25) Churchill, M. R.; Missert, J. R., to be submitted for publication.

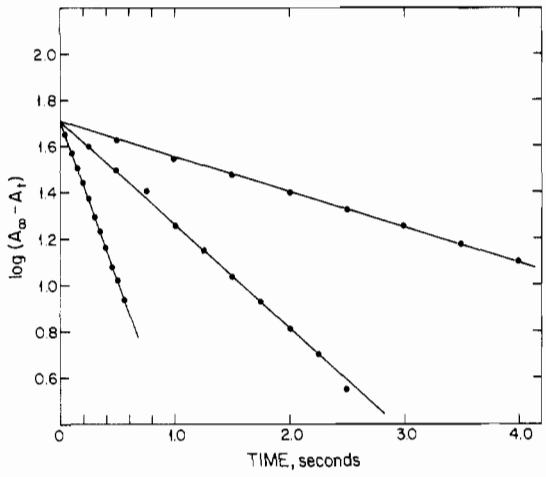

Figure 4. Typical first-order plots for $[(ENCA)CuCl]_4O_2$ product formation in the oxidation of $[(ENCA)_2CuCl]_2$ by dioxygen ($10^2 \times [[(ENCA)_2CuCl]_2] = 1.0$–$2.5$ M, $10^3[O_2]_0 = 0.35$ M, nitrobenzene solvent, 48.7 °C, reaction monitored at 700 nm).

of excess py. Needless to say, these tetranuclear oxidation products are highly active phenolic oxidative coupling initiators. They give the products of eq 1b presumably because they readily coordinate deprotonated phenolic substrates, which would favor C–C coupling rather than C–O coupling (reaction 1a).[3,7,13]

The evidence for the formation of different product structures will be useful in discussing the kinetic results of the next section.

Kinetics of Oxidation. Practical Considerations. As indicated above, copper(I) complexes with py and ENCA are generally less soluble than are those with DENC.[15] Solubility determines the upper limit of copper(I) concentration that can be investigated kinetically under homogeneous conditions. The lower limit is set by the stoichiometric requirement that $[Cu^I_T]_0 \geq 40[O_2]_0$ for the maintenance of pseudo-first-order conditions, together with the need for an absorbance change on reaction that is large enough to give precise kinetic data. At $L/Cu^I_T = 1.0$ the characteristics of the various ligand–copper(I) halide combinations are such that only one new system, that with ENCA–copper(I) chloride in nitrobenzene, could be studied at a sufficiently high copper(I) concentration to ensure pseudo-first-order conditions. This system was investigated with $[Cu^I_T] = (1.8$–$6.0) \times 10^{-2}$ M between 11.5 and 41.0 °C.

Four new systems were found practical at $L/Cu^I_T = 2.0$, namely, with L = py, X = Cl, $[Cu^I_T] = (1.0$–$80.0) \times 10^{-2}$ M (12.3–49.0 °C) in nitrobenzene and in methylene chloride (20.1 °C),[26] with L = ENCA, X = Cl, $[Cu^I_T] = (2.0$–$24.0) \times 10^{-2}$ M in nitrobenzene (15.5–46.6 °C), and with L = ENCA, X = Br, $[Cu^I_T] = (1.6$–$5.4) \times 10^{-2}$ M in nitrobenzene (52.0–87.0 °C).

Reaction Order in $[O_2]$. For the above systems, plots of ln $(A_\infty - A_t)$ vs. time, where A_t is the absorbance of the $L_4Cu_4X_4O_2$ product at time t, were linear for at least 4 half-lives. A typical set of plots is given in Figure 4. Extrapolation of these plots to zero time gave no evidence for reactant preequilibria.[15] At fixed $[Cu^I_T]$, $[L]/[Cu^I_T]$, and temperature, the pseudo-first-order rate constant, k_{obsd}, was independent of $[O_2]_0$ in the range $(0.2$–$2.1) \times 10^{-3}$ M and monitoring wavelength between 500 and 850 nm. These results show that the oxidation reaction is first order in $[O_2]$ and that reaction intermediates either are not formed in significant concentrations or do not absorb appreciably in the wavelength range 500–850 nm.[15]

(26) The solubility of this system in methylene chloride dramatically decreases with decreasing temperature, which greatly reduces the range of $[Cu^I_T]$ that can be investigated at lower temperatures. The order of reaction changes with $[Cu^I_T]$ in this system (see text), but the ranges of $[Cu^I_T]$ available at temperatures less than ca. 20 °C were too small to give precise data. Since methylene chloride boils at 40.1 °C and a wide temperature range is desirable for the calculation of accurate activation parameters, we wish to report data only at 20.1 °C for this system at this time.

Table IV. Kinetic Data for Oxidation of $[L_mCuX]_4$ Complexes by Dioxygen in Nitrobenzene

complex	temp[a]	k_T[b]	k_T-(calcd)[b,c]	$\Delta H^\ddagger_T$[c,d]	$-\Delta S^\ddagger_T$[c,e]
$[(ENCA)CuCl]_4$	11.5	20.0	19.4	4.4 ± 0.2	37 ± 1
	22.0	27.0	26.4		
	31.0	32.0	33.9		
	41.0	45.0	44.1		
$[(ENCA)_2CuCl]_4$	16.0	83.5	81.3	4.3 ± 0.2	35 ± 1
	22.4	95.4	97.9		
	29.5	121	119		
	42.4	159	167		
	45.5	186	180		
$[(ENCA)_2CuBr]_4$	52.0	2.4	2.1	5.7 ± 0.3	40 ± 1
	65.0	2.8	3.0		
	74.0	4.1	4.1		
	87.0	5.4	5.4		
$[(py)_2CuCl]_4$	12.3	520	580	2.9 ± 0.2	36 ± 1
	19.9	730	679		
	28.3	840	800		
	37.5	917	950		

[a] Given in °C. [b] Units are M^{-1} s^{-1} with a maximum standard deviation of ±5%. [c] Calculated from a nonlinear least-squares fit of the data to eq 10 with temperature as an independent variable,[19] errors shown are 1 standard deviation. [d] Units are kcal mol^{-1}. [e] Units are cal deg^{-1} mol^{-1} at 25.0 °C.

Kinetics of Oxidation of $[(ENCA)CuCl]_4$. At $[ENCA]/[Cu^I_T] = 1.0$ and fixed temperature, plots of k_{obsd} vs. $[Cu^I_T]$ were linear and passed through the origin, indicating that the reaction is first order in $[Cu^I_T]$. This same reaction order was found for oxidation of $[(DENC)CuX]_4$ (eq 4), whose tetranuclear constitutions were independently established.[15] Structural similarities between monodentate DENC and ENCA ligands make it very likely that the reactant at the molar ratio $ENCA/Cu^I_T = 1.0$ is $[(ENCA)CuCl]_4$, with $[[(ENCA)CuCl]_4] = [Cu^I_T]/4$ under all experimental conditions (eq 8). $[(ENCA)CuCl]_4$ shows no tendency to dissociate to give dimeric species under any of the conditions investigated. Values of the second-order rate constant k_T as a function of temperature are listed in Table IV, together with calculated k_T values obtained by a nonlinear least-squares determination of the activation parameters from a fit of the data to eq 8 with temperature as an independent variable.[19]

$$d[[(ENCA)CuCl]_4O_2]/dt = k_T[[(ENCA)CuCl]_4][O_2] \quad (8)$$

Kinetics of Oxidation at $L/Cu^I_T = 2.0$. Second-order rate laws for oxidation under pseudo-first-order conditions should give values of $k_{obsd}/[Cu^I_T] = k_T$ that are independent of $[Cu^I_T]$, as found in the DENC[15] and ENCA (Table IV) systems at $L/Cu^I_T = 1.0$. Figure 5 shows a plot of $k_{obsd}/[Cu^I_T]$ vs. $[Cu^I_T]$ for data obtained with $[py]/[Cu^I_T] = 2.0$ at 20.1 °C in nitrobenzene. The ratio $k_{obsd}/[Cu^I_T]$ is independent of $[Cu^I_T]$ at $[Cu^I_T] \gtrsim 60 \times 10^{-3}$ M, showing that the oxidation reaction is first order in $[Cu^I_T]$ at concentrations above this limit, where tetrameric $[(py)_2CuCl]_4$ predominates (Table I). Cryoscopic measurements at $[Cu^I_T] = 2.8 \times 10^{-2}$ m, near the midrange of $[Cu^I_T]$ for which $k_{obsd}/[Cu^I_T]$ is a linear function of $[Cu^I_T]$ (Figure 5), show that dimeric $[(py)_2CuCl]_2$ predominates under these conditions. The change of reaction order with increasing $[Cu^I_T]$ is thus ascribed to association of dimeric species to give tetramers (eq 9).

$$2[L_2CuX]_2 \overset{K_9}{\rightleftharpoons} [L_2CuX]_4 \quad (9)$$

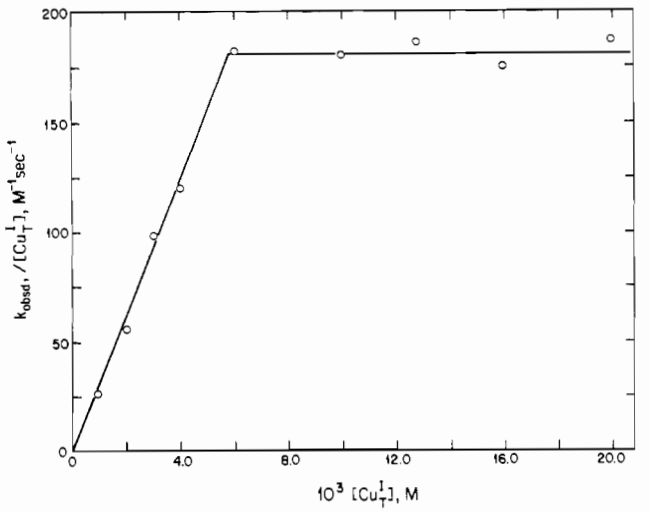

Figure 5. Plot of $k_{obsd}/[Cu^I_T]$ vs. $[Cu^I_T]$ for the oxidation of chloro(pyridine)copper(I) species by dioxygen at $py/Cu^I_T = 2.0$ in nitrobenzene at 20.1 °C. The two regions of the plot correspond to reactions of $[(py)_2CuCl]_2$ (low $[Cu^I_T]$) and $[(py)_2CuCl]_4$ (high $[Cu^I_T]$), respectively.

We would expect, from the results presented above and our previous work,[15] that tetrameric species $[L_2CuX]_4$ would react with O_2 according to rate law 10, which is clearly the case in

$$d[[LCuX]_4O_2]/dt = k_T[[L_2CuX]_4][O_2] \quad (10)$$

the py–Cu^I_T system at $[Cu^I_T] \gtrsim 60 \times 10^{-3}$ M (Figure 5). The linear dependence of $k_{obsd}/[Cu^I_T]$ at lower $[Cu^I_T]$, where dimeric $[L_2CuX]_2$ complexes predominate, corresponds to rate law 11. Plots of the same form as that in Figure 5 in the

$$d[[LCuX]_4O_2]/dt = k_D[[L_2CuX]_2]^2[O_2] \quad (11)$$

$ENCA/Cu^I_T = 2.0$ system were used to determine the $[Cu^I_T]$ ranges over which alternative rate laws 10 and 11 are obeyed. The results were consistent with the cryoscopic data in Tables I and II.

Kinetics of Tetramer Oxidation at $L/Cu^I_T = 2.0$ in Nitrobenzene. Equation 10 was obeyed under the following conditions: L = ENCA, X = Cl, $[Cu^I_T] = (6.0–32.5) \times 10^{-2}$ M (16.0–45.5 °C); L = ENCA, X = Br, $[Cu^I_T] = (1.6–5.4) \times 10^{-2}$ M (52.0–87.0 °C); L = py, X = Cl, $[Cu^I_T] = (6.0–20.0) \times 10^{-2}$ M (12.3–37.5 °C). In each case $[[L_2CuX]_4] = [Cu^I_T]/4$. The plot of k_{obsd} vs. $[[(ENCA)_2CuCl]_4]$ in Figure 6 illustrates the fit of typical data to eq 10. Observed values of k_T are compared in Table IV with those calculated from a nonlinear least-squares determination of the activation parameters in eq 10 with temperature as an independent variable.[19]

The fact that eq 10 is obeyed at lower $[Cu^I_T]$ and higher temperatures with L = ENCA and X = Br instead of X = Cl indicates that $[(ENCA)_2CuBr]_4$ is more thermodynamically stable than $[(ENCA)_2CuCl]_4$ in eq 9. It is worth noting that $[(DENC)CuBr]_4$ tetramers also persist at lower $[Cu^I_T]$ than those employed in kinetic studies of $[(DENC)CuCl]_4$ oxidation.[15] Another useful observation is that the $[Cu^I_T]$ range over which eq 10 is obeyed with X = Cl is practically the same at all temperatures investigated; this indicates that reaction 9 has only a slight temperature dependence and substantiates the use of cryoscopic molecular weight measurements in nitrobenzene as a means of establishment of copper(I) reactant molecularities.

A comparison of kinetic data for oxidation of tetrameric copper(I) reactants $[L_mCuX]_4$ (m = 1, 2; X = Cl, Br) is made in Table V. Consider first the data for X = Cl, m = 1. Replacing DENC with ENCA causes a 1.8-fold increase in k_T at 25.0 °C in nitrobenzene, with low $\Delta H^‡$ and very negative

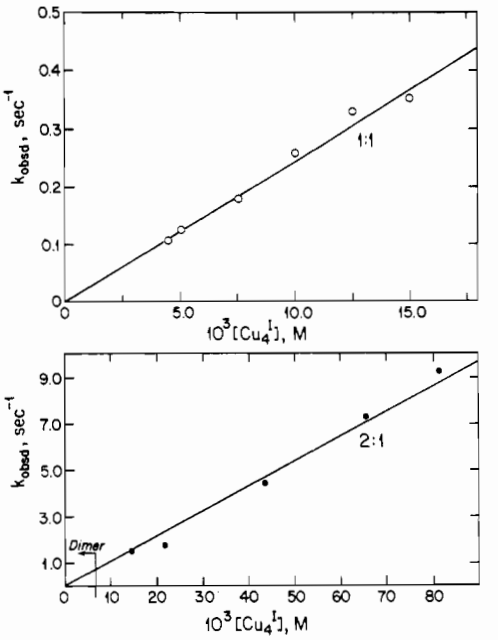

Figure 6. Plots of k_{obsd} vs. $[Cu^I_4]$, where $[Cu^I_4]$ represents $[[(ENCA)CuCl]_4]$ and $[[(ENCA)_2CuCl]_4]$ in the upper and lower sections, respectively. The solvent is nitrobenzene at 22.2 °C. Note the different concentration ranges required to observe copper(I) tetramer oxidation at $L/Cu^I_T = 1.0$ and $L/Cu^I_T = 2.0$. The onset of kinetic and cryoscopic behavior characteristic of dimer oxidation occurs at the concentration marked in the lower section.

Table V. Comparison of Kinetic Data for Oxidation of $[L_mCuX]_4$ Complexes by Dioxygen in Aprotic Solvents[a]

L	m	k_T[b]	$\Delta H^‡$[c]	$-\Delta S^‡$[d]
		(a) X = Cl		
py	2	770	2.9	36
ENCA	1	28	4.4	37
	2	110	4.3	35
DENC[e]	1	15	3.9	40
		6.9[f]		
		5.4[g]	2.1	48
		(b) X = Br		
ENCA	2	1.2	5.7	40
DENC[e]	1	0.58	5.9	40

[a] Solvent is nitrobenzene except where stated. [b] Units are M^{-1} s^{-1} at 25.0 °C. [c] Units are kcal mol^{-1} (typical uncertainty ±0.3 unit). [d] Units are cal deg^{-1} mol^{-1} at 25.0 °C (typical uncertainty ±1 unit). [e] Data from ref 15. [f] Solvent is methylene chloride. [g] Solvent is benzene.

$\Delta S^‡$ observed in both systems. There is a further 4-fold *increase* in k_T when one additional ENCA ligand is coordinated to each copper(I) center in $[(ENCA)CuCl]_4$. Also, at 25.0 °C $[(py)_2CuCl]_4$ reacts 7 times faster with O_2 than does $[(ENCA)_2CuCl]_4$. Finally, replacing X = Cl with X = Br has a general decelerating effect, but the effect of replacing DENC with two ENCA ligands is much smaller when X = Br.

These results strongly support the dioxygen insertion mechanism proposed earlier for oxidation of $[(DENC)CuX]_4$ complexes[15] for the following reasons: (a) $[(ENCA)_2CuCl]_4$ would be expected to react more slowly with O_2 if attack of the oxidant on one of the four copper(I) centers were necessary for reaction to occur, but the opposite effect is observed, and there is no spectral or kinetic evidence for the involvement of reaction precursors; (b) the progressive rate increases that occur on increasing the L/Cu^I ratio and on replacing ENCA with py are consistent with a most facile dioxygen insertion process for L = py, presumably because it is the hardest of this series of ligands.[27]

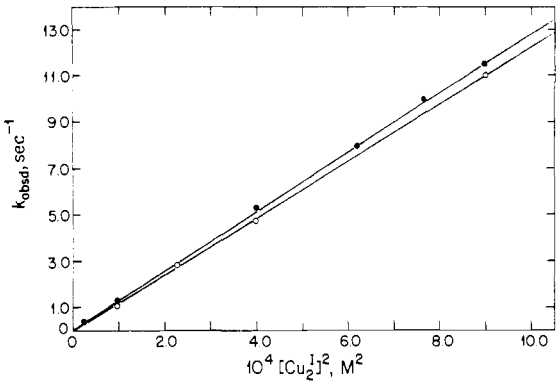

Figure 7. Dependence of the observed pseudo-first-order rate constant k_{obsd} on $[(py)_4Cu_2Cl_2]^2$ at (○) 20.1 and (●) 48.7 °C for oxidation of dimeric species. Note the very small temperature dependence of the slope, which gives the overall third-order rate constant k_D.

The observed activation enthalpy, $\Delta H^{\ddagger}_T$, for oxidation is definitely smaller for $[(py)_2CuCl]_4$ than for other tetrameric chloro(pyridine)copper(I) species (Table V). An increase of electron density from coordinated ligands evidently increases the repulsive forces within the tetrahedron of halogen atoms at the core of these copper(I) species, thus facilitating dioxygen insertion in the rate-determining step.

In an earlier section we assembled evidence for different product core structures I and II and now wish to consider how such differences might arise.

Increased electron density from coordinated ligands will not only facilitate O_2 insertion but will also accelerate electron transfer from copper(I).[28] The transfer from copper(I) centers of the minimum of three electrons necessary to break the O–O bond only after complete core penetration is indicated by the results for $L_4Cu_4X_4$ oxidation with L = DENC or ENCA: the products are $(\mu\text{-O})_2L_4Cu_4X_4$ species, structure I, whose μ-oxo groups must obviously be outside the halo core, explaining the ease with which reaction 3 occurs.

The transfer of three or more electrons *before* complete core penetration by O_2 accounts for structure II with L = py. Tetrameric halocopper(I) complexes with harder ligands will presumably be found to react aprotically with dioxygen in the same fashion.

Kinetics of Dimer Oxidation at $L/Cu^I_T = 2.0$. Equation 11 was obeyed under the following conditions, with X = Cl throughout: L = ENCA, $[Cu^I_T] = (1.0\text{–}5.0) \times 10^{-2}$ M (15.5–46.6 °C, nitrobenzene); L = py, $[Cu^I_T] = (1.0\text{–}5.0) \times 10^{-2}$ M (12.7–49.0 °C, nitrobenzene); L = py, $[Cu^I_T] = (4.5\text{–}20.0) \times 10^{-2}$ M (20.1 °C, methylene chloride[26]). The dimer concentration is given by $[Cu^I_T]/2$ in each experiment. It is evident that dimeric $[(py)_2CuX]_2$ species persist at higher $[Cu^I_T]$ in methylene chloride than in nitrobenzene. The plot of k_{obsd} vs. $[[(py)_2CuCl]_2]^2$ in Figure 7 illustrates a typical fit of the data to eq 11. Table VI lists observed values of k_D (M^{-2} s^{-1}), together with calculated values from a nonlinear least-squares determination of activation parameters in eq 11 with temperature as an independent variable.[19] A comparison of $L_4Cu_2Cl_2$ kinetic oxidation data is made in Table VII.

The dimer $[(py)_2CuCl]_2$ reacts with O_2 about 5 times more rapidly than does $[(ENCA)_2CuCl]_2$ in nitrobenzene at 25.0 °C; a similar ratio of rate constants for oxidation of the corresponding tetramers (eq 10) is observed (Table V), although this is probably circumstantial, as presumably is the 1.4 kcal mol^{-1} difference in $\Delta H^{\ddagger}$ (Tables V and VII) (see below). Oxidation of $[(py)_2CuCl]_2$ is 7–10 times slower in methylene chloride and pyridine[30] than it is in nitrobenzene; this is a much larger kinetic solvent effect than was observed for oxidation of $[(DENC)CuCl]_4$ via the insertion mechanism[15] (Table V).

Two mechanisms are consistent with rate law 11. The first consists of eq 9 and 12, where Cu^I_2 denotes dimeric $[L_2CuCl]_2$

$$2Cu^I_2 \underset{}{\overset{K_9}{\rightleftharpoons}} Cu^I_4 \qquad (9)$$

$$Cu^I_4 + O_2 \xrightarrow{k_T} Cu^{II}_4O_2 \qquad (12)$$

species and Cu^I_4 the corresponding tetramers. Here, eq 9 is the rapid dimer–tetramer equilibrium considered earlier and eq 12 is the characteristic process for tetramer oxidation governed by k_T (Table V). This mechanism assumes that only tetramers are oxidizable and that the measured third-order rate constant will be given by $k_D = k_TK_9$. Values of K_9 can be calculated with $K_9 = k_D/k_T$ from the data in Tables V and VII. At 25.0 °C we calculate $K_9 \approx 30$ and 20 M^{-1} for L = ENCA and py, respectively, in nitrobenzene. An example will serve to show that the predictions of the above mechanism are inconsistent with the data. Figure 5 indicates that eq 10 is obeyed at $[Cu^I_T] \gtrsim 60 \times 10^{-3}$ M in the pyridine system. If at least 90% of Cu^I_T is in tetrameric form at this lower limit, then K_9 must be at least 1500 M^{-1}, which is 75 times larger than the predicted value.[31] Since eq 10 also is obeyed at $[Cu^I_T] \gtrsim 60 \times 10^{-3}$ M with L = ENCA, we discard the

Table VI. Kinetic Data for Oxidation of $[L_2CuCl]_2$ Complexes in Nitrobenzene

complex	temp[a]	$10^{-3} \times k_D$[b]	$10^{-3}k_D$ (calcd)[b,c]	$\Delta H^{\ddagger}_D$[c,d]	$-\Delta S^{\ddagger}_D$[c,e]
$[(ENCA)_2CuCl]_2$	15.5	2.90	2.88	1.4 ± 0.1	38 ± 1
	21.4	3.05	3.09		
	32.0	3.40	3.49		
	34.1	3.70	3.57		
	46.6	4.04	4.07		
$[(py)_2CuCl]_2$	12.7	15.0	15.0	0.0 ± 0.2	39 ± 1
	28.0	15.7	15.8		
	36.9	16.5	16.3		
	49.0	16.9	17.0		
	20.1[f]	1.8			

[a] Given in °C. [b] Units are M^{-2} s^{-1} with a maximum standard deviation of ±5%. [c] Calculated from a nonlinear least-squares fit of the data to eq 11 with temperature as an independent variable,[19] errors shown are 1 standard deviation. [d] Units are kcal mol^{-1}. [e] Units are cal deg^{-1} mol^{-1} at 25.0 °C. [f] Solvent is methylene chloride (see text).

Table VII. Comparison of Kinetic Data for Oxidation of $L_4Cu_2Cl_2$ Complexes by Dioxygen in Aprotic Solvents[a]

L	$10^{-3}k_D$[b]	$\Delta H^{\ddagger}$[c]	$-\Delta S^{\ddagger}$[d]
ENCA	3.1	1.4	38
py	15.0	0.0	39
py[e]	1.8		
py[f]	1.3		

[a] Solvent is nitrobenzene except where stated. [b] Units are M^{-2} s^{-1} at 25.0 °C. [c] Units are kcal mol^{-1}. [d] Units are cal deg^{-1} mol^{-1} at 25.0 °C. [e] Solvent is methylene chloride; temp = 20.1 °C. [f] Solvent is pyridine; reactant might have $n > 4$ (data from ref 30; see ref 35).

(27) It is also possible that steric inhibition of O_2 insertion is responsible, at least in part, for the lower rate constant for oxidation of $[(ENCA)_2CuCl]_4$, although the rate constant difference for $[(ENCA)_mCuCl]_4$ (m = 1 or 2) makes this appear unlikely; in addition, the amido substituents in $[(DENC)CuI]_4$ are well removed from the faces through which insertion must occur.[15]

(28) One of the characteristics of copper(I) centers is their stabilization by soft, electron-withdrawing ligands.[10,29]

(29) Patterson, G. S.; Holm, R. H. *Bioinorg. Chem.* **1975**, *4*, 257.

(30) Hopf, F. R.; Rogic, M. M.; Wolf, J. F., submitted for publication in *J. Phys. Chem.*

(31) K_9 = 20 M^{-1} actually predicts that $[[(py)_2CuCl]_4]$ is only 6.3×10^{-3} M at $[Cu^I_T] = 60 \times 10^{-3}$ M in nitrobenzene at 25.0 °C.

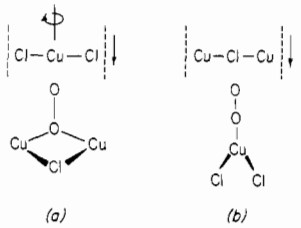

Figure 8. Hypothetical activated complex for dimer oxidation via eq 13 and 14. Ligands are omitted. The lower species is a weak reaction precursor (eq 13) whose Cu–Cu axis is depicted orthogonal to that of a second dimer. View b is along the Cu–Cu axis of the precursor. Insertion of the O–O group through the four-membered ring of the upper dimer may be rate determining.

mechanism consisting of eq 9 and 12 for both ligand systems.

The second alternative mechanism, eq 13 and 14, simply

$$Cu^{I}_2 + O_2 \overset{K_{13}}{\rightleftharpoons} Cu_2O_2 \qquad (13)$$

$$Cu_2O_2 + Cu^{I}_2 \xrightarrow{k_{14}} Cu^{II}_4O_2 \qquad (14)$$

reverses the order of events. Here, eq 13 represents a rapid equilibrium between the reactants and a precursor and the second-order rate constant k_{14} governs the rate determining reaction of this precursor with dimeric copper(I). This mechanism predicts that the observed first-order rate constant will be given by eq 15. If $K_{13}[Cu^{I}_2] \lesssim 0.1$ at the highest $[Cu^{I}_2]$

$$k_{obsd} = \frac{K_{13}k_{14}[Cu^{I}_2]^2}{1 + K_{13}[Cu^{I}_2]} \qquad (15)$$

employed, then $K_{13} \lesssim 4$, 3, and 1 M^{-1} in the $[(ENCA)_2CuCl]_2$ (nitrobenzene), $[(py)_2CuCl]_2$ (nitrobenzene), and $[(py)_2CuCl]_2$ (methylene chloride) systems, respectively, at 20 °C.[32] Bis(pyridine) copper(I) dimers evidently have little affinity for O_2 in eq 13, consistent with the lack of evidence for any reaction precursors. Under these circumstances $k_D = K_{13}k_{14}$, a composite parameter, for this mechanism.

The appearance of ligand-dependent product structures I or II from copper(I) dimer oxidation is accounted for as follows. Whatever its constitution (ranging from $Cu^{I}_2O_2$ to $Cu^{II}_2O^{-II}_2$), the precursor Cu_2O_2 is of low stability. We visualize step 14 in Figure 8. Here, the precursor is assigned a structure in which only one oxygen atom is coordinated to the copper centers.[33] The fact that k_D is greatest for $[(py)_2CuCl]_2$ oxidation in nitrobenzene (Table VII) may be due to K_{13} being largest in this system (a polar precursor would be relatively destabilized by a low-polarity solvent like methylene chloride[34]). As envisioned, step 14 consists of partial or complete insertion of the uncoordinated oxygen atom of the precursor through the Cu(X,X)Cu face of a copper(I) dimer.[20] As we have seen, insertion reactions are most facile in tetrameric $[(py)_2CuCl]_4$ species (Table V) and the same presumably holds for the corresponding dimers. If insertion precedes the minimum three-electron transfer necessary to break the O–O bond, then the product will have structure II. On the other hand, electron transfer before insertion will, after rearrangement and ligand loss (eq 5), give the $(\mu\text{-}O)_2L_4Cu_4X_4$ species, structure I. It is unfortunate that actual values of K_{13} cannot be obtained from the kinetic data; the prospects of determining K_{13} by other means are not good if for no other reason that the precursors are apparently so weak.

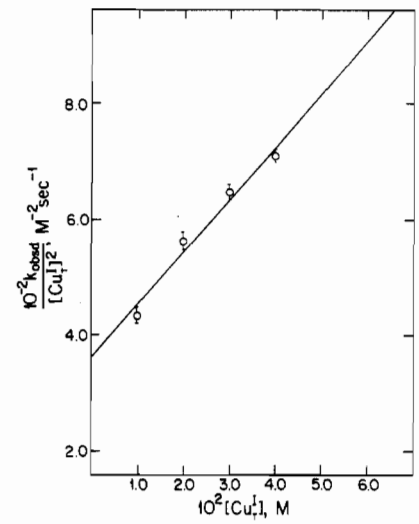

Figure 9. Plot of $k_{obsd}/[Cu^{I}_T]^2$ vs. $[Cu^{I}_T]$ for oxidation of chloro(pyridine)copper(I) species by dioxygen in methylene chloride at 20.1 °C. The linear dependence arises from oxidation of monomeric $(py)_2CuCl$ species (see eq 16).

Similar activated complexes are probably present at the point at which electron transfer from copper(I) to O_2 occurs in these dimer and tetramer oxidation reactions. Formal insertion is not necessarily rate determining in dimer oxidation (compare $\Delta H^{\ddagger}$ in Tables V and VII), the O_2 molecule "assembling" the activated complex from the two dimers necessary for irreversible electron transfer.

Kinetics of Oxidation at $py/Cu^{I}_T = 2.0$ in Methylene Chloride. As noted in the previous section, the kinetic data for this system fit eq 11 for dimer oxidation up to near the limit of solubility, $[Cu^{I}_T] = 20 \times 10^{-2}$ M at 20 °C, consistent with a lower relative stability of tetrameric $[(py)_2CuCl]_4$ species in methylene chloride than in nitrobenzene (eq 9).

An interesting phenomenon is observed at $[Cu^{I}_T] \lesssim 4 \times 10^{-2}$ M in that $k_{obsd}/[Cu^{I}_T]^2$ becomes a linear function of $[Cu^{I}_T]$ (Figure 9), consistent with the requirements of eq 16. Here,

$$k_{obsd} = A[Cu^{I}_T]^2 + B[Cu^{I}_T]^3 \qquad (16)$$

A and B are the intercept and slope, respectively, of Figure 9. Although A is much less precise than B, the stoichiometric relationship $k_D = 4A = 1.5 \times 10^3$ M^{-2} s^{-1} is in acceptable agreement with the estimate of k_D in eq 11 at much higher copper(I) concentrations (Table VI). The second term in eq 16 corresponds to rate law 17 for oxidation of monomeric

$$d[[LCuX]_4O_2]/dt = k_M[(py)_2CuCl]^3[O_2] \qquad (17)$$

species $(py)_2CuCl$, which can be accounted for by the mechanism given by eq 18–20.

$$2(py)_2CuCl + O_2 \overset{K_{18}}{\rightleftharpoons} [(py)_2CuCl]_2O_2 \qquad (18)$$

$$[(py)_2CuCl]_2O_2 + (py)_2CuCl \xrightarrow{k_{19}} X \qquad (19)$$

$$X \xrightarrow[(py)_2CuCl]{fast} \text{products} \qquad (20)$$

This mechanism predicts that the observed first-order rate constant, k_{obsd}, will be given by eq 21. If $K_{18}[(py)_2CuCl]^2 \lesssim 0.1$ at the highest $[(py)_2CuCl]$ for which eq 16 applies, then $K_{18} \lesssim 50$ M^{-2} in eq 18 at 20 °C. This assumption leads to

(32) This statement arises from the fact that the methylene chloride system could only be investigated near 20 °C. The upper limits for K_{13} evidently also apply at higher temperatures in nitrobenzene (see text).

(33) For a discussion of alternative M_2O_2 interactions, see, for example: Klotz, I. M.; Duff, L. L.; Kurtz, D. M.; Shriver, D. F. In "Invertebrate Oxygen-Binding Proteins"; Lamy, J., Lamy, J., Eds.; Dekker: New York, 1981; p 469.

(34) The dielectric constants of methylene chloride and nitrobenzene are 8.93 and 34.82, respectively, at 25 °C.

(35) The data of Hopf et al.[30] exhibit a decrease in reaction order at $[Cu^{I}_T] \gtrsim 8 \times 10^{-2}$ M, in that the reaction appears to be second order in $[Cu^{I}_T]$ above this concentration limit. If it is assumed that copper(I) chloride is entirely dimeric at $[Cu^{I}_T] \gtrsim 8 \times 10^{-2}$ M in pyridine at 25 °C, then $k_D = 1.3 \times 10^3$ M^{-2} s^{-1}. This estimate is similar to the rate constant for oxidation of $(py)_4Cu_2Cl_2$ in methylene chloride (Table VII), but the reactant could conceivably have 5-coordinate copper(I) centers with pyridine in such large excess.

$$k_{obsd} = \frac{K_{18}k_{19}[(py)_2CuCl]^3}{1 + K_{18}[(py)_2CuCl]^2} \quad (21)$$

$k_M = K_{18}k_{19}$ in eq 17, where k_{19} governs rate-determining transfer of a third electron into the weak precursor $[(py)_2CuCl]_2O_2$. The nature of the product X in eq 19 is unknown, but very rapid reaction of X with $(py)_2CuCl$ is required to account for the measured stoichiometry and kinetics.

Hopf et al.[30] have recently measured the kinetics of oxidation of excess dissolved copper(I) chloride by dioxygen in pyridine at 25 °C. The data fit eq 22 at $[Cu^I_T] \lesssim 8 \times 10^{-2}$ M and give

$$\frac{d[product]}{dt} = k_M[(py)_mCuCl]^3[O_2] \quad (22)$$

$k_M = (7 \pm 2) \times 10^3$ M^{-3} s^{-1} in pyridine at 25 °C. This rate constant compares well with $k_M = (9 \pm 1) \times 10^3$ M^{-3} s^{-1} calculated from the slope of Figure 9 for the reaction of $(py)_2CuCl$ with O_2 in methylene chloride at 20 °C.

The evidence for a term that is third order in $[Cu^I_T]$ is significant because it demonstrates the need for the transfer of at least three electrons from pyridine–copper(I) centers to O_2 before these systems can become irreversible; this condition is necessary for rupture of the O–O bond and results in the formation of oxocopper(II) species. The hypothetical precursors in eq 13 and 18 may both have the structure suggested in Figure 8. The major obvious difference between the tetramer, dimer, and monomer oxidation systems is that no insertion process is called for in the last system.

Relevance to Phenolic Oxidative Coupling. Previous work provides indirect evidence for copper(I)–phenol complex formation in some copper-catalyzed phenolic oxidative coupling sysems.[3,13] Such interactions would be expected to favor lower copper(I) aggregates and thereby alter the $[Cu^I_T]$ ranges over which rate law 10, 11, or 16 applies in the absence of substrate, as well as perhaps affect the respective magnitudes of k_T, k_D, and B. However, these minor variations are to be expected only if oxocopper(II) products still appear in phenol–copper(I) oxidation.

The alternatives to the above include a situation in which, because of phenol–copper(I) interactions, the complete reduction of O_2 does not occur before phenol oxidation. For example, a dimeric $(phenol)_mL_nCu_2X_2$ species might produce $(phenol)_xL_yCu_2X_2O_2$ on reaction with O_2, with rate law 23.

$$d[product]/dt = k_p[(phenol)_mL_nCu_2X_2][O_2] \quad (23)$$

Here, k_p is a phenol-dependent second-order rate constant, to be contrasted with the third-order rate constant k_D observed in the absence of phenol at comparable $[Cu^I_T]$. Completion of the catalytic cycle (oxidation of phenol and production of water, eq 1) would be facilitated if $(phenol)_mL_nCu_2X_2O_2$ had well-developed negative charge on the oxygen atoms, which could then deprotonate coordinated phenol and thereby promote its oxidation. However, because of the redox stoichiometry of the $(phenol)_mL_nCu_2X_2O_2$ intermediate, we would only be dealing with –I as the lowest possible oxidation state of oxygen (as a formal peroxide), and such centers are undoubtedly less basic than their counterparts in oxocopper(II) species. In addition, the O–O bond has already been broken in the formation of the latter.

The purpose of this last section is to point out that the effects of phenol–copper(I) complexation can, in principle, be observed kinetically on the basis of the work reported here. Our efforts to assemble a molecular mechanism for copper-catalyzed phenolic oxidative coupling reactions are continuing.

Acknowledgment. This work was financially supported by Biomedical Research Grant RR07143 from the Department of Health and Human Services and Faculty Research Grant 7590 from Northeastern University, which are gratefully acknowledged. We also thank Leslie Root and Edward Witten for experimental assistance and Drs. John Hutchinson, Milorad Rogič, and James wolf for valuable discussions and for the provision of results prior to publication.

Registry No. $(ENCA)_4Cu_2Cl_2$, 85049-01-0; $(ENCA)_8Cu_4Cl_4$, 85066-75-7; $(py)_4Cu_2Cl_2$, 82409-65-2; $(py)_8Cu_4Cl_4$, 85049-02-1; $[(ENCA)CuCl]_4O_2$, 85049-03-2; $[(ENCA)CuBr]_4O_2$, 85049-04-3; $[(ENCA)CuCl]_4(CO_3)_2$, 85049-05-4; $(py)_3Cu_4Cl_4O_2$, 85049-06-5; $(py)_4Cu_4Cl_4O_2$, 85049-07-6; $(py)_4Cu_4Cl_6O$, 18716-93-3; $[(DENC)CuCl]_4O_2$, 80105-85-7; $[(DENC)CuBr]_4O_2$, 80105-86-8; $[(DENC)CuCl]_4(CO_3)_2$, 85066-76-8; $[(DENC)CuBr]_4(CO_3)_2$, 85049-08-7; $(py)_4Cu_4Br_6O$, 19477-99-7; $[(ENCA)CuCl]_4$, 85049-09-8; $[(ENCA)_2CuBr]_4$, 85049-10-1; Cu, 7440-50-8; phenol, 108-95-2.